

Chemical and Physical Modifications of Electrospun Keratin Nanofibers Induced by Heating Treatments

Alessio Varesano,¹ Claudia Vineis,¹ Cinzia Tonetti,¹ Diego Omar Sánchez Ramírez,² Giorgio Mazzuchetti¹

¹Institute for Macromolecular Studies, National Research Council of Italy (CNR-ISMAL), Corso Giuseppe Pella 16, I-13900 Biella, Italy

²Politecnico di Torino, Department of Applied Science and Technology, Corso Duca degli Abruzzi 24, I-10129 Turin, Italy

Correspondence to: A. Varesano (E-mail: a.varesano@bi.ismac.cnr.it)

ABSTRACT: In this study, we aimed to examine the effects of heating treatments on wool-derived keratin nanofibers obtained by electrospinning. Interestingly, the keratin nanofibers did not lose their nanofibrous shape at high temperatures. On the contrary, the diameter of keratin nanofibers significantly decreased after heating. Even the chemical structure of the keratin was not significantly altered by heating, as observed by IR spectroscopy, except for a shoulder at 1720 cm^{-1} and the amide III band. The spectral feature changes matched the formation of crosslinking amide bonds between protein chains well. Moreover, for various applications, it is essential that nanofibers are stable in water. Heating treatments were carried out at different temperatures and times to assess what heating conditions gave the keratin nanofibers water stability. Finally, no significant changes in the thermal behavior were observed in the samples after heating treatments compared to the untreated keratin nanofibers; this was a sign of negligible or slight degradations of the protein chains. © 2014 Wiley Periodicals, Inc. *J. Appl. Polym. Sci.* **2014**, *131*, 40532.

KEYWORDS: biopolymers & renewable polymers; crosslinking; electrospinning; porous materials; proteins

Received 3 October 2013; accepted 31 January 2014

DOI: 10.1002/app.40532

INTRODUCTION

Between nonfood proteins, keratin is the most abundant, being the major component of wool, feather, hair, horns, and nails.¹ So, keratin wastes represent an important renewable source of biopolymers that can be exploited. Keratin extracted from wool has many useful properties, including biocompatibility and biodegradability,² and it supports the growth and adhesion of fibroblasts³ and osteoblasts.⁴ Thus, keratin is expected to be applicable for biomedical use in a similar manner to collagen and fibroin. Moreover, keratin materials can absorb toxic substances, such as heavy-metal ions,⁵ formaldehyde, and other volatile organic compounds (VOCs), so that possible applications can also be foreseen in water purification and air cleaning. Inorganic pollutants, such as heavy-metal ions, are more dangerous because of their high toxicity and are most often persistent and difficult to biodegrade. Therefore, the determination of alternative and economically viable substitutes to the currently used active carbon adsorbents to remove toxic metal ions is needed.⁶

Because of its low molecular weight (65–11 kDa) and its poor mechanical properties, regenerated keratin is very fragile and difficult to handle. Recently, extracted keratin has been regenerated in films from ionic liquids by the addition of methanol, ethanol, and water as coagulation solvents,⁷ and keratin-based

microparticles have been produced by spray-drying and tested as drug-delivery systems.⁸ Keratin has been used for the production of nanofibers by electrospinning.^{9,10}

The electrospinning process is a low-cost and simple method for producing nanofibrous materials that have particular properties such as a high surface-to-volume ratio and a high porosity; this makes them promising candidates for several applications, such as filter membranes,¹¹ cell-growth scaffolds,¹² wound dressings,¹³ and drug-delivery vehicles.¹⁴ In applications such as liquid filtration and biomedical fields, water stability is required.

It has been recently reported¹⁵ that keratin nanofibers showed good stability in water after a heating treatment at 180°C . In this study, keratin nanofibers were subjected to heating treatments at different temperatures and times to assess what heating temperatures and times gave keratin nanofibers water stability. Moreover, this study provided new evidence to support the hypothesis that heating is responsible for the formation of crosslinking amide bonds between carboxylic and amine side-chain groups of the amino acids. Interestingly, we also found that heating significantly reduced the diameter of the nanofibers and did not alter the thermal behavior of the electrospun keratin.

Table I. Mass-Loss Measurements

Sample	Weight loss (%)
120°C, 1 h	0.00
120°C, 2 h	0.01
120°C, 4 h	0.03
150°C, 1 h	3.86
150°C, 2 h	5.07
150°C, 4 h	6.29
180°C, 1 h	8.66
180°C, 2 h	12.1
180°C, 4 h	13.4

EXPERIMENTAL

Keratin Extraction and Purification

Keratin was extracted from wool by sulfitolysis with sodium metabisulfite.¹⁶ Preliminarily, the wool fibers were cleaned by Soxhlet extraction with petroleum ether to remove fatty matter and washed with distilled water. An amount of 15 g of cleaned fibers were cut into snippets and treated with 300 mL of a solution containing urea (8M) and Na₂S₂O₅ (0.5M) adjusted to pH 6.5 with NaOH (5N) under shaking for 2 h at 65°C. The mixture was filtered with 30- μ m and then 5- μ m pore-size filters, and the keratin aqueous solution obtained was dialyzed against distilled water with a cellulose tube (3.500-Da molecular weight cutoff) for 3 days at room temperature, with the distilled water changed frequently. The keratin solution was frozen and then lyophilized with a Heto PowerDry PL3000 freeze dryer to obtain soluble keratin powder.

Electrospinning

Freeze-dried keratin powder was dissolved in formic acid (reagent grade, >95%, Sigma-Aldrich) at room temperature under magnetic stirring overnight (ca. 16 h) at a concentration of 15% w/w. The keratin solutions were electrospun into nanofibers with a typical electrospinning setup. A plastic syringe was filled with about 4 mL of solution. The solution was pushed at a 0.003 mL/min flow rate by a high-precision syringe pump (KDS200, KD Scientific, Inc.) through a stainless steel tip with an internal diameter of 0.2 mm connected to the syringe. The tip was electrically connected to a generator (SL50, Spellman High Voltage Electronics Corp.), which supplied a voltage of 25 kV. A stainless steel plate (20 \times 20 cm²) was placed in front of the tip at a distance 15 cm as a nanofiber collector. The collector was electrically grounded. During electrospinning, the environmental conditions were recorded every minute with an Escort RH iLog data-logger. The temperature was 23.1 \pm 0.5°C, and the relative humidity (RH) was 36.7 \pm 1.1%. The nanofibers were collected for 60 \pm 5 min for each sample.

Heating Treatments and Nanofiber Characterization

The electrospun keratin nanofiber samples were subjected to heating treatments in an oven at different temperatures (i.e., 120, 150, and 180°C) and times (i.e., 1, 2, and 4 h). Hereinafter, the samples are labeled as “xxx°C, y h,” where xxx is the temperature in degrees Celsius of the heating treatment and y is the duration in hours. The nanofiber samples not subjected to

heating are labeled “as spun.” The nanofiber samples were stored for at least 24 h at 20°C and 65% RH before heating treatments.

The mass loss related to the heating treatments was measured by means of thermogravimetric analysis (TGA) with a Mettler Toledo TGA-DSC 1. About 0.5 mg of the keratin nanofibers were put in a 70-mL aluminum oxide crucible for each analysis. The nanofibers were dried at 105°C to a constant mass. Then, isothermal runs were performed at the same temperatures as the heating treatments (i.e., 120, 150, and 180°C), and the weight was continuously recorded by the instrument. The calorimeter cell was flushed with air at 70 mL/min. The TGA data were elaborated with a Mettler Toledo STARE system.

The thermal behavior of the keratin nanofibers was studied by TGA with the same TGA instrument and software. The calorimeter cell was flushed with gas at 70 mL/min (nitrogen or air). About 1.5 mg of nanofibers was put in a 70-mL aluminum oxide crucible for each analysis. The runs were performed from 30 to 700°C with a heating rate of 20°C/min. Derivative thermogravimetry (DTG) was used to identify the temperature of maximum mass-loss rates.

The nanofiber samples were stored for at least 24 h at 20°C and 65% RH before each characterization.

The nanofiber samples were put in deionized water for 24 h to assess what heating temperatures and times gave them stability to water. The samples were then dried for at least 24 h at 20°C and 65% RH on paper sheets.

The morphology of the nanofibers was observed by scanning electron microscopy (SEM). SEM investigations were performed with an LEO 435 VP scanning electron microscope (Leica Electron Optics with an acceleration voltage of 15 kV at about a 24-mm working distance). The nanofiber samples were sputter-coated with a 20 nm thick gold layer in rarefied argon (20 Pa) with an Emitech K550 sputter coater, with a current of 20 mA for 180 s, to improve the image quality. Nanofiber diameter measurements were carried out on different SEM images with GIMP 2.8.2 (GNU Image Manipulation Program) as image software. The average and standard deviation values were calculated on 50 measures for each sample. A heteroscedastic Student's *t* test was used to calculate the two-tailed test *p* values to statically evaluate the effect of the heating treatments on the average nanofiber diameter.

IR spectra were recorded with a Thermo Nicolet Nexus spectrometer by an attenuated total reflection technique with a Smart Endurance accessory (with a diamond crystal ZnSe focusing element) in the range from 4000 to 550 cm⁻¹ with 100 scans and a 4-cm⁻¹ band resolution. Omnic 6.2 software (by Thermo Electron) was used to perform attenuated total reflection baseline correction.

RESULTS AND DISCUSSION

Mass Loss During the Heating Treatments

During heating treatments, the keratin nanofibers were subjected to mass loss depending on the heating conditions. The mass-loss measurements are reported in Table I. Because the nanofibers were exsiccated before the mass-loss evaluation, these

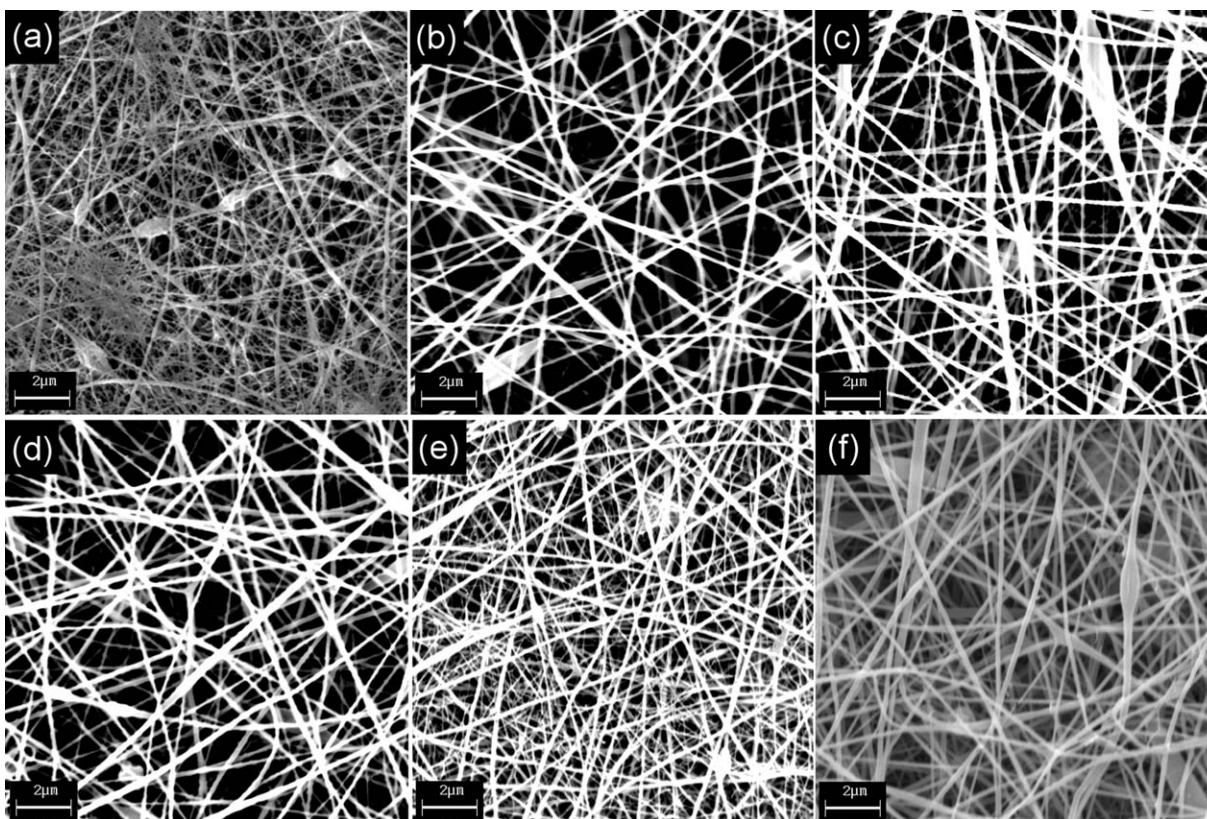


Figure 1. SEM pictures of the electrospun keratin nanofibers: (a) as spun and after thermal treatments (b) at 120°C for 4 h, (c) at 150°C for 4 h, (d) at 180°C for 1 h, (e) at 180°C for 2 h, and (f) at 180°C for 4 h.

changes were related to the production of volatile molecules because of protein degradation and chemical reactions (e.g., condensation reaction). Further discussions on the mass loss can be found in the following sections.

Nanofiber Morphology After Heating Treatments

Electrospun keratin nanofibers were observed by SEM before and after the heating treatments. Some of the SEM pictures are reported in Figure 1. Figure 1(a) related to the electrospun keratin before heating shows nanofibers with few beads, ramification, and beltlike structures. The fibrous structure was not altered by the heating treatments, as shown in Figure 1(b–f), and the same defects observed in the samples before the heating treatments were still present after heating.

The average nanofiber diameter was measured for all of the samples. The results are reported in Table II. Before the heating treatments, the electrospun keratin nanofibers had a diameter of 158 nm. As the temperature and time increased, the average diameter decreased. Treatments at 150°C for at least 2 h and at 180°C for at least 1 h reduced the average nanofiber diameter to about 130 nm; this corresponded to an 18% decrease. The assumption that the nanofibers were cylinders, and because there was a density of 1.27 g/cm³ for the keratin nanofibers,¹⁷ the specific surface area of the nanofibers before heating was 19.9 m²/g, whereas for nanofibers after heating, it was 24.2 m²/g, with an increase of 21.6%.

A Student *t* test was carried out to assess the statistical significance of the difference between the as-spun sample and the samples after

heating treatments. The resulting *p* values are reported in Table II. In particular, there was a significant difference ($p < 0.01$) in the average diameters of the samples subjected to temperatures of 150°C or higher (i.e., samples treated at 150°C for 2 h, 150°C for 4 h, 180°C for 1 h, 180°C for 2 h, and 180°C for 4 h) and the nanofibers not subjected to heating treatments (as-spun sample).

Water Stability Assessment

All of the samples of electrospun keratin nanofibers (before and after heating treatments) were put in deionized water for 24 h to study their behavior in water. It is known¹⁵ that heating enhances this kind of stability, but a screening of the heating temperatures and times that gave the keratin nanofibers this property was still missing.

Figure 2 shows the SEM pictures of some of the samples tested. Figure 2(a), which refers to the untreated sample, shows that the electrospun mats completely lost their porosity. Some nanofibrous structures were still visible, but they were glued each other to form a filmlike layer. This was because the untreated electrospun keratin nanofibers swelled and were partially dissolved in water.

Similar results were obtained on samples treated at 120 and 150°C. In particular, Figure 2(b,c) is related to the samples treated for 4 h (the longest duration for the heating treatments) at 120 and 150°C, respectively. On the contrary, after the treatments at 180°C, the electrospun mats still maintained a nanofibrous, porous structure, even when the nanofibers appeared flattened and deformed to some extent, as shown in

Table II. Average Diameters and Student *t* Test Results Based on 50 Measurements

Sample	Average diameter (nm)	<i>p</i> value
As spun	158 ± 38	—
120°C, 1 h	154 ± 33	>0.1
120°C, 2 h	162 ± 52	>0.1
120°C, 4 h	143 ± 40	0.06
150°C, 1 h	146 ± 30	0.07
150°C, 2 h	129 ± 26	<0.01
150°C, 4 h	127 ± 29	<0.01
180°C, 1 h	133 ± 37	<0.01
180°C, 2 h	134 ± 31	<0.01
180°C, 4 h	136 ± 48	<0.01

Figure 2(d–f); this was related to the samples heated at 180°C for 1, 2, and 4 h.

IR Analysis

IR analysis was carried out to study the chemical modifications induced by the heating of the electrospun keratin. Figure 3 shows the spectra of all of the samples before and after the heating treatments. The spectra of the electrospun keratin nanofibers shown in Figure 3(a) were characterized by the absorption bands related to peptide bonds. The amide A band

at 3310 cm^{-1} was assigned to the stretching vibrations of N–H bonds, the amide I band at 1650 cm^{-1} was assigned to the stretching vibrations of C=O bonds, the amide II at 1540 cm^{-1} was assigned to the in-plane bending modes of N–H bonds with some contributions of C–N stretching vibrations, and the amide III at 1200 cm^{-1} was a complex band assigned to an in-phase combination of N–H in-plane bending, C–N stretching vibrations, C–C stretching, and C=O bending vibrations,¹⁸ but it also depended on the nature of the side-chain groups and hydrogen bonding.¹⁹ Finally, the intense peak at 1025 cm^{-1} was attributed to the stretching vibrations of the Bunte's salt residues.²⁰

All of the spectra in Figure 3 appeared to be similar, except for the shoulder at 1720 cm^{-1} and shown in Figure 3(b) and the intensity and position of the second peak of the amide III band in Figure 3(c). The shoulder at 1720 cm^{-1} progressively decreased as the heating treatments became stronger. This shoulder was attributed¹⁷ to the stretching vibrations of the C=O bonds of the terminal-free carboxylic groups of the protein and side-chain carboxylic groups in amino acids, such as glutamic acid and aspartic acid. Keratin, also after electrospinning, is particularly rich in the two amino acids with a concentration of 14.4 mol % in glutamic acid and a concentration of 8.67 mol % in aspartic acid.¹⁵

Figure 3(c) shows changes in the amide III spectral features as the strength of the heating treatments increased. In particular, the peak at lower wave numbers decreased in intensity and

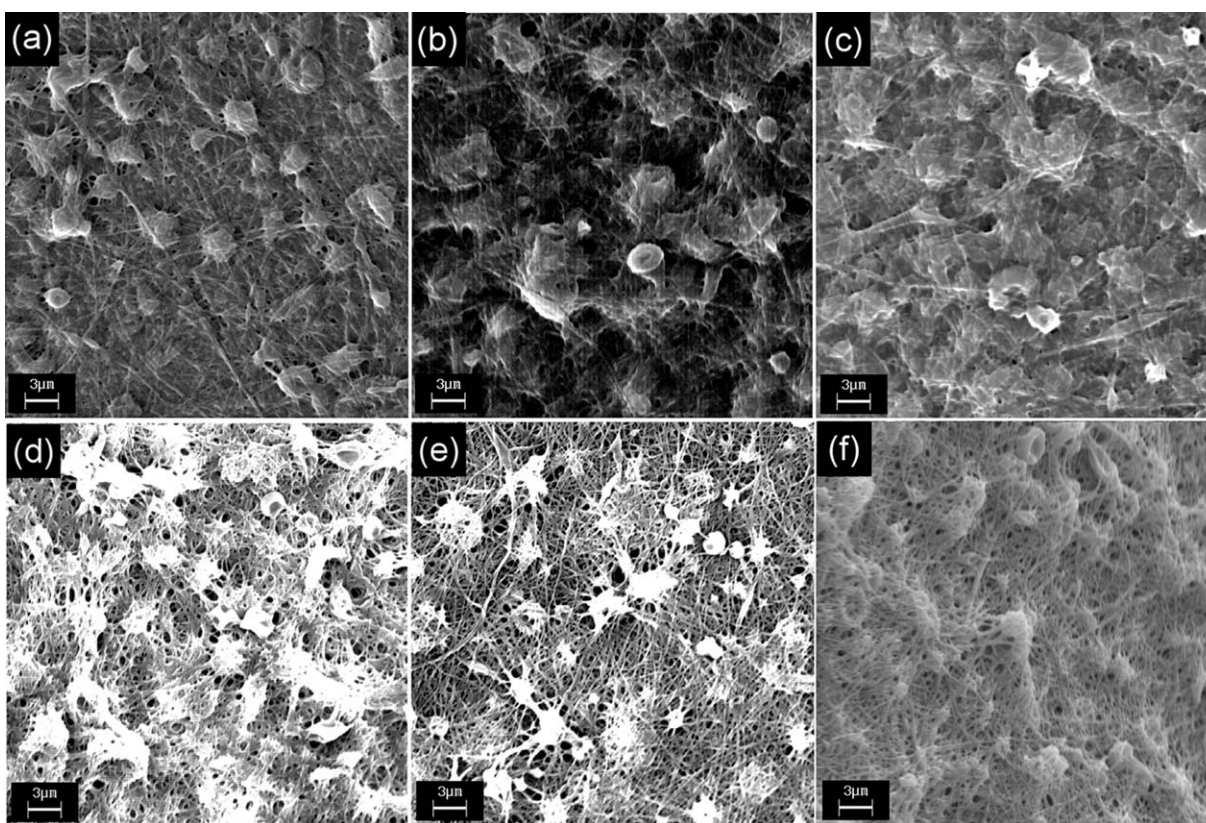


Figure 2. SEM pictures of the electrospun keratin nanofibers (a) as spun and after thermal treatments (b) at 120°C for 4 h, (c) at 150°C for 4 h, (d) at 180°C for 1 h, (e) at 180°C for 2 h, and (f) at 180°C for 4 h after contact with water for 24 h.

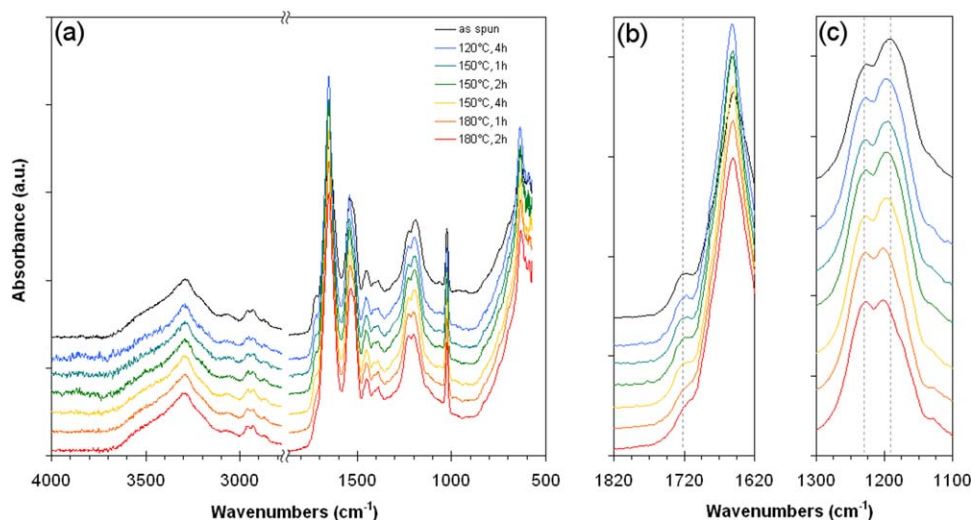


Figure 3. IR spectra of the electrospun keratin nanofibers before and after heating treatments: (a) spectra from 4000 to 2800 cm^{-1} and from 1800 to 550 cm^{-1} , (b) details of the spectra for the region centered to 1720 cm^{-1} (assigned to carboxylic groups), and (c) details of the spectra for the region centered to the amide III band at 1200 cm^{-1} . [Color figure can be viewed in the online issue, which is available at wileyonlinelibrary.com.]

shifted to higher wave numbers. The amide III was particularly sensitive to changes in the protein secondary structure.^{21,22} Therefore, conformational modifications could explain the spectral changes observed, but no significant changes were observed in amide I, as should be when the protein secondary structural changes. This was in agreement with the observations of a previous work.¹⁵ On the other hand, the amide III band also depended on the nature of the side-chain groups and hydrogen bonding.¹⁹ Chemical groups containing several amine groups, such as diamine and guanidine, can have IR absorption bands in the region between 1150 and 1250 cm^{-1} .^{23,24} Thus, another possible explanation for the spectral changes in the amide III band could have been that chemical reactions involving the side-chain groups of some amino acids should have contributed to some extent to the alteration of the amide III band. In particular, among amino acids, arginine had one imino nitrogen and two amine groups in the guanidine moiety. Arginine is highly present in wool and keratin-based products; in electrospun keratin nanofibers, arginine is present at a concentration of 6.16 mol %.¹⁵ Hence, a crosslinking reaction involving acid (e.g., glutamic acid and aspartic acid) and base (e.g., arginine) side-chain groups of amino acids could explain both the spectral feature changes induced by the high-temperature treatments on electrospun keratin nanofibers. Moreover, the literature reported that a reaction process at high temperature stabilized the chicken feather fiber structure, probably by the crosslinking of the protein chains by the reaction of the amine and carboxyl side-chain groups.²⁵ This hypothesis was in agreement with the measures of mass loss during the heating treatments reported previously (Table I). The mass losses observed were related to both the degradation of heat-sensitive amino acids and the production of water by the reaction of amine and carboxyl groups. A slight increase in the ratio between the heat-resistant and heat-labile amino acids in thermally treated keratin nanofibers was already reported.¹⁵ On the other hand, the formation of volatile molecules as products of condensation reactions is

another possibility in the consideration of the enhancement of the water stability induced by heating treatments. In fact, the water stabilization of proteins by heating depends on the nature of the protein itself. Some proteins show increased solubility after heating, and other proteins show improved stability after heating. In particular, stabilization is favored by (1) the formation of a high number of nondisulfide covalent crosslinking bonds and (2) slight degradation of the protein chains.²⁶

Thermal Behavior of the Nanofibers

TGA was carried out under nitrogen and in air to investigate the thermal behavior of the electrospun keratin nanofibers after heating treatments. For the sake of brevity, in Figures 4 and 5, the TGA curves of two treated samples (viz., at 150°C for 2 h and at 180°C for 2 h) were compared with the as-spun sample. The thermogravimetric data are listed in Table III.

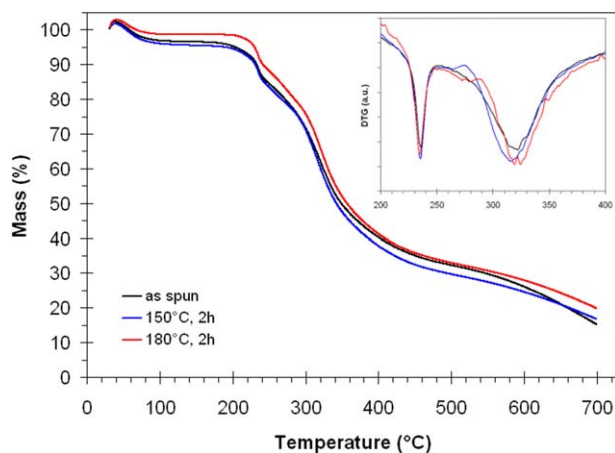


Figure 4. Thermogravimetric curves of the electrospun keratin nanofibers as spun and after heating treatments at 150°C for 2 h and at 180°C for 2 h under nitrogen. The inset shows DTG. [Color figure can be viewed in the online issue, which is available at wileyonlinelibrary.com.]

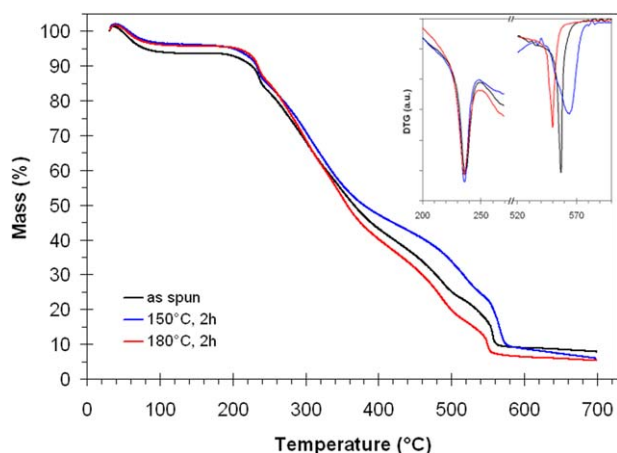


Figure 5. Thermogravimetric curves of the electrospun keratin nanofibers as spun and after heating treatments at 150°C for 2 h and at 180°C for 2 h in air. The inset shows DTG. [Color figure can be viewed in the online issue, which is available at wileyonlinelibrary.com.]

No significant alterations in the thermal behavior were observed on the thermally treated samples compared to the untreated sample. In particular, the TGA curves obtained under nitrogen in Figure 4 show that there was a mass loss below 100°C, and this was attributed to the absorbed water. The major thermal degradation happened between 200 and 400°C. As DTG analysis revealed, this degradation consisted of two main steps. The first step was quite a fast process, with a maximum mass-loss rate at about 235°C for all of the samples. The second degradation step was broad and reached the maximum mass-loss rate at about 320°C. Then, the curves became rather flat, with a decrease in the slope as the temperature increased above 450°C. The main difference observed in the thermogravimetric data from the TGA curves under nitrogen was the residual mass at 700°C (Table III), which increased as the temperature of the heating treatment increased.

In air, the TGA curves (Figure 5) again showed a mass loss below 100°C; this was probably due to water evaporation. Also in this case, the degradation process was composed of two main steps. The first step occurred at the same temperature observed under nitrogen, and therefore, we supposed that this degradation step should not involve oxygen. On the contrary, the second degrada-

Table III. Data from TGA Under Nitrogen and Air

Gas	Sample	Temperature of maximum mass-loss rate from DTG (°C)		Residual mass at 700°C (%)
		First step	Second step	
N ₂	As spun	235.9	322.6	15.2
	150°C, 2 h	234.9	317.5	16.7
	180°C, 2 h	235.0	323.7	19.8
Air	As spun	235.6	554.5	7.8
	150°C, 2 h	235.3	565.4	5.8
	180°C, 2 h	236.0	548.5	5.3

tion step was a fast thermooxidative exothermic process (this information was obtained from differential scanning calorimetry traces not reported here), which occurred at a higher temperature with maximum mass-loss rates in the range from 548 to 565°C. There was no clear correlation between heating treatments and the temperatures of the maximum thermooxidative degradation rates of the samples. After the thermooxidative degradation step, the curves became flat. The residual masses at 700°C after TGA in air (reported in Table III) were close each other. However, it seemed that the residual mass decreased slightly as the temperature of the heating treatments increased.

CONCLUSIONS

The major component of wool, feather, hair, horns, and nails is keratin, a nonfood protein characterized by the high amount of sulfur because of the presence of cysteine residues. Keratin is the most abundant nonfood protein that can be exploited in several high-technology applications thanks to its useful properties: biocompatibility, biodegradability, and the absorption of harmful chemical compounds (e.g., heavy-metal ions, dyes, formaldehyde, and other VOCs). Electrospinning keratin-based nanofibers with a small diameter and high specific surface promote keratin properties. The results demonstrate that the post-electrospinning heating treatment did not destroy the nanoscale fibrous structure and could even improve the properties of keratin nanofibers with interesting technological outcomes. In particular, heating (at temperature of 150°C or higher) produced a reduction of the nanofiber diameter (with an increase in the surface area of about 22%) and gave stability to water without worsening thermal behavior. Moreover, the IR spectroscopy results suggest that the high-temperature heating gave rise to a chemical reaction involving the amine and carboxyl side-chain groups of some amino acids and likely produced crosslinking amide bonds.

ACKNOWLEDGMENTS

This work was supported by the NanoTWICE project (Progetto Bandiera–La Fabbrica del Futuro; FdF-SP1-T1.2), which was funded by the Programma Nazionale della Ricerca (2011–2013) of the Ministero dell’Istruzione dell’Università e della Ricerca (Italy).

REFERENCES

- Fraser, R. D. B.; MacRae, T. P.; Rogers, G. E. *Keratins: Their Composition, Structure and Biosynthesis*; Thomas: Springfield, IL, **1972**; p 23.
- Yamauchi, K.; Maniwa, M.; Mori, T. *J. Biomater. Sci. Polym. Ed.* **1998**, *9*, 259.
- Tachibana, A.; Furuta, Y.; Takeshima, H.; Tanabe, T.; Yamauchi, K. *J. Biotechnol.* **2002**, *93*, 165.
- Tachibana, A.; Kaneko, S.; Tanabe, T.; Yamauchi, K. *Biomaterials* **2005**, *26*, 297.
- Aluigi, A.; Tonetti, C.; Vineis, C.; Tonin, C.; Mazzuchetti, G. *Eur. Polym. J.* **2011**, *47*, 1756.
- Ali, I. *Sep. Purif. Rev.* **2010**, *39*, 95.
- Li, R.; Wang, D. *J. Appl. Polym. Sci.* **2013**, *127*, 2648.

8. Cilurzo, F.; Selmin, F.; Aluigi, A.; Bellosta, S. *Polym. Adv. Technol* **2013**, *24*, 1025.
9. Yuan, J.; Shen, J.; Kang, I. K. *Polym. Int.* **2008**, *57*, 1188.
10. Aluigi, A.; Varesano, A.; Montarsolo, A.; Vineis, C.; Ferrero, F.; Mazzuchetti, G.; Tonin, C. *J. Appl. Polym. Sci.* **2007**, *104*, 863.
11. Gopal, R.; Kaur, S.; Ma, Z.; Chan, C.; Ramakrishna, S.; Matsuura, T. *J. Membr. Sci.* **2006**, *281*, 581.
12. Min, B. M.; Lee, G.; Kim, S. H.; Nam, Y. S.; Lee, T. S.; Park, W. H. *Biomaterials* **2004**, *25*, 1289.
13. Uppal, R.; Ramaswamy, G. N.; Arnold, C.; Goodband, R.; Wang, Y. *J. Biomed. Mater. Res. Part B: Appl. Biomater.* **2011**, *97*, 20.
14. Jin, H. J.; Fridrikh, S. V.; Rutledge, G. C.; Kaplan, D. L. *Biomacromolecules* **2002**, *3*, 1233.
15. Aluigi, A.; Corbellini, A.; Rombaldoni, F.; Zoccola, M.; Canetti, M. *Int. J. Biol. Macromol.* **2013**, *57*, 30.
16. Aluigi, A.; Zoccola, M.; Vineis, C.; Tonin, C.; Ferrero, F.; Canetti, M. *Int. J. Biol. Macromol.* **2007**, *41*, 266.
17. Aluigi, A.; Tonetti, C.; Vineis, C.; Tonin, C.; Mazzuchetti, G. *Eur. Polym. J.* **2011**, *47*, 1756.
18. Cardamone, J. M. *Int. J. Biol. Macromol.* **2008**, *42*, 413.
19. Jackson, M.; Mantsch, H. H. *Crit. Rev. Biochem. Mol. Biol.* **1995**, *30*, 95.
20. Erra, P.; Gómez, N.; Dolcet, L. M.; Juliá, M. R.; Lewis, D. M.; Willoughby, J. H. *Text. Res. J.* **1997**, *67*, 397.
21. Cai, S. W.; Singh, B. H. *Biochemistry* **2004**, *43*, 2541.
22. Liu, H.; Yu, W. *J. Appl. Polym. Sci.* **2007**, *103*, 1.
23. Forbes, M. W.; Bush, M. F.; Polfer, N. C.; Oomens, J.; Dunbar, R. C.; Williams, E. R.; Jockusch, R. A. *J. Phys. Chem. A* **2007**, *111*, 11759.
24. Jones, W. J.; Orville-Thomas, W. J. *Trans. Faraday Soc.* **1959**, *55*, 193.
25. Senoz, E.; Wool, R. P.; McChalicher, C. W. J.; Hong, C. K. *Polym. Degrad. Stab.* **2012**, *97*, 297.
26. Mohammed, Z. H.; Hill, S. E.; Mitchell, J. R. *J. Food Sci.* **2000**, *65*, 221.